ISSN: 2414-1895 DOI: 10.6919/ICJE.202505_11(5).0034

Investigation of the Morphology of PCL-Based Electrospun Nanofibers under Different Experimental Parameters

Jiaqi Jiang, Xiaohong Chen, Tianming Lu, and Honglei Zhou*

School of Materials and Chemistry, University of Shanghai for Science and Technology, Shanghai 200093, China

Abstract

This research examines how changes in concentration, flow rate, and the inclusion of various additives impact the morphological characteristics of electrospun nanofibers derived from polycaprolactone (PCL). These factors play a critical role in determining fiber diameter, surface features, and overall quality. The study systematically assesses the effects of these variables on the size, shape, and consistency of the nanofibers. Findings reveal that fine-tuning these parameters allows for the tailored design of fiber properties to meet specific requirements. For example, adjustments in concentration significantly alter fiber formation and structural integrity, whereas flow rate is closely linked to the diameter and uniformity of the fibers. Incorporating certain additives further improves the functional performance of the nanofibers. The outcomes of this work contribute essential knowledge for refining the electrospinning process of PCL-based nanofibers, establishing both a theoretical framework and practical evidence for their use in biomedical applications, filtration technologies, and packaging solutions.

Keywords

Core-Shell Structure; Coaxial Electrospinning; Polycaprolactone; Nanoparticles.

1. Introduction

The fabrication of nanofibers has increasingly relied on electrospinning, a technique that has gained widespread recognition [1]. In this process, a polymer solution at the needle tip is exposed to high voltage, creating an electric field. This exposure generates a surface charge on the liquid. Once the voltage exceeds a critical level, the internal repulsive forces of the solution overpower its surface tension, causing the ejection of a charged jet. At the spinneret, this jet forms a Taylor cone, resulting in the production of fibers at the nano- or micro-scale [2]. During collection, the solvent evaporates, and the fibers are deposited onto a collector.

As an innovative material, electrospun nanofiber membranes possess a three-dimensional framework, customizable porosity, and a pliable texture with superior elasticity [3]. These features provide them with unique benefits in various fields. For example, their high surface area relative to volume and porous nature make them exceptionally effective in filtration, enabling the efficient capture of tiny particles [4]. Additionally, the mechanical and functional properties of these membranes can be improved by integrating various additives [5].By introducing specific compounds, their hydrophobicity, water resistance, and mechanical durability can be significantly enhanced [6]. These qualities highlight the extensive potential applications of electrospun nanofiber membranes in areas such as healthcare, energy, and protective equipment.

Polycaprolactone (PCL), a biocompatible and biodegradable polymer, is extensively utilized in biomedical applications, including drug delivery, tissue engineering, and filtration systems, owing to its favorable properties [7]. Electrospinning, a versatile method capable of producing nanofibers with

ISSN: 2414-1895 DOI: 10.6919/ICJE.202505_11(5).0034

a high surface area-to-volume ratio and adjustable porosity, has attracted considerable attention in the development of PCL-based materials [8]. The morphology and characteristics of electrospun PCL nanofibers are largely influenced by processing parameters such as polymer concentration, flow rate, and the inclusion of additives [9].

Research has demonstrated that polymer concentration plays a significant role in the electrospinning process and the resulting fiber morphology [10]. Flow rate is critical in determining the consistency and quality of the fibers [11]. The addition of nanoparticles or other polymers as additives can further improve the functionality and performance of the fibers [12].

This study systematically examines the impact of polymer concentration, flow rate, and additives on the morphology of PCL-based electrospun nanofibers. A thorough analysis of the resulting fibers offers valuable insights into how these parameters affect fiber properties. Understanding these influences is crucial for optimizing the electrospinning process to produce nanofibers with tailored characteristics for specific applications, such as tissue engineering scaffolds or high-efficiency filtration materials [13].

2. Experimental Section

2.1 Materials

Polycaprolactone (PCL, Mn = 80,000) and Zinc Oxide nanoparticles (n-ZnO, Mn = 81.39, 99.9% metals basis, particle size: 30 ± 10nm) were acquired from Shanghai Macleans Biochemical Technology Co., Ltd. in Shanghai, China. Additionally, nano hydroxyapatite (nHAp, Mn = 502.31), Gelatin (Gel), 1,1,1,3,3,3-Hexafluoro-2-propanol (HFIP, C3H2F6O, 99%) were sourced from Sinopharm Chemical Reagent Co., Ltd., also located in Shanghai, China. None of these chemical reagents underwent further purification prior to the formulation of the spinning solution.

2.2 Preparation of Single-Fluid Electrospinning

Preparation of PCL Spinning Solutions:PCL spinning solutions were prepared by dissolving 0.5 g, 1.0 g, 1.5 g, and 2.0 g of PCL granules in 10 mL of hexafluoroisopropanol (HFIP) solvent, respectively. The mixtures were stirred continuously for 12 hours in a constant-temperature water bath maintained at 50°C until the solutions became colorless and transparent. These solutions were labeled as F1, F2, F3, and F4, respectively.

Preparation of PCL-n-ZnO Spinning Solutions:To prepare PCL-n-ZnO spinning solutions, 0.05 g, 0.1 g, 0.2 g, and 0.3 g of n-ZnO powder were added to fully dissolved 10% (w/v) PCL solutions. Prior to mixing, the n-ZnO powder was ultrasonicated for 20 minutes to ensure uniform dispersion. The mixtures were then stirred for 12 hours in a constant-temperature water bath at 50°C. These solutions were designated as F5, F6, F7, and F8, respectively.

Preparation of PCL-Gel-n-ZnO Spinning Solutions:For the PCL-Gel-n-ZnO spinning solutions, 0.66 g, 0.42 g, 0.25 g, and 0.11 g of gelatin (Gel) were added to fully dissolved 10% (w/v) PCL solutions containing 0.5% (w/v) n-ZnO. The mixtures were stirred for 12 hours in a constant-temperature water bath at 50°C. These solutions were labeled as F9, F10, F11, and F12, respectively.

Electrospinning Process:The prepared PCL spinning solutions were loaded into 20 mL syringes and mounted onto a syringe pump. A single-needle spinneret was installed and connected to a high-voltage electrospinning device using an alligator clip. A layer of silicone oil paper was placed on the rotating drum collector, positioned 16 cm from the needle tip, to facilitate the collection of deposited fibers. The feed rate for single-fluid electrospinning was set to 1 mL/h. The experiments were conducted under controlled environmental conditions, with a temperature of 25 ± 3°C and a relative humidity of 45 ± 5%.

ISSN: 2414-1895 DOI: 10.6919/ICJE.202505_11(5).0034

2.3 Preparation of Single-Fluid Electrospinning

Preparation of PCL-nHAp spinning solution: Add 0.2 g of nHAp powder to a fully dissolved 10% PCL (w/v) solution. The nHAp powder is subjected to ultrasonic treatment for 20 minutes before use. The mixture is then heated and stirred in a water bath at 50°C for 12 hours.

Preparation of PCL-Gel-n-ZnO spinning solution: Dissolve 1 g of PCL particles, 0.25 g of Gel particles, and 0.05 g of n-ZnO, as well as 1.5 g of PCL particles and 0.2 g of nHAp, respectively, in 10 mL of HFIP. Heat and stir the mixture in a water bath at 50°C for 12 hours until the solution becomes a white liquid with no particulate matter at the bottom. The solution is then set aside for further use.

Initially, the prepared 10% PCL (w/v) and 15% PCL (w/v) spinning solutions are loaded into separate 20-mL syringes. The coaxial spinning nozzle is connected to a high-voltage direct current generator using alligator clips. The experimental parameters are listed in Table 1. Specifically, a voltage of 5 kV is applied to the coaxial electrospinning setup. The experiments are conducted at a temperature of 25 ± 3°C and a relative humidity of 45 ± 5%. The influence of different flow rate ratios on fiber morphology is investigated, yielding nanofibers F13-F18. The detailed experimental parameters are shown in the table.

Table 1. Parameters for Coaxial Electrospinning Experiments

Number	Core layer Solution	Shell layer solution	Core layer flow rate(mL/h)	Shell layer flow rate(mL/h)
F13	10%PCL-Gel(8:2)-0.5ZnO	15%PCL-2%nHAp	1	1
F14	15%PCL-2%nHAp	10%PCL-Gel(8:2)-0.5ZnO	1	1
F15	15%PCL-2%nHAp	10%PCL-Gel(8:2)-0.5ZnO	0.5	1
F16	15%PCL-2%nHAp	10%PCL-Gel(8:2)-0.5ZnO	0.5	1.5
F17	15%PCL-2%nHAp	10%PCL-Gel(8:2)-0.5ZnO	1	0.5
F18	15%PCL-2%nHAp	10%PCL-Gel(8:2)-0.5ZnO	1.5	0.5

2.4 Observation of Nanofiber Morphology

The nanofiber products F1-F12, prepared by single-fluid electrospinning, and the nanofiber products F13-F18, created through coaxial electrospinning, were dried in an oven at 40°C for 12 hours to remove the solvent from the fiber surfaces. A small portion of the fibers was then cut and adhered to a sample stage using conductive adhesive. The samples were gold-coated for 90 seconds in a nitrogen atmosphere to enhance their conductivity. The surface morphology of the fibers was observed using a Quanta FEG450 field emission scanning electron microscope.

3. Results and Discussion

3.1 Morphological Analysis of Single-Fluid Electrospun Nanofibers

In this study, we initially designed single-fluid electrospinning using PCL solutions of different concentrations (F1: 5%, F2: 10%, F3: 15%, and F4: 20%) and observed the morphology of the collected nanofibers using SEM. As shown in Figure 1 (a-d), F1 exhibited a large number of beads. With increasing concentration, the beads disappeared. Both F2 and F3 displayed smooth and uniform fiber morphologies. However, when the concentration increased to 20%, the fibers in F4 became uneven in thickness and began to exhibit bending. Therefore, based on these results, we selected concentrations of 10% and 15% as the appropriate spinning windows.

ISSN: 2414-1895 DOI: 10.6919/ICJE.202505_11(5).0034

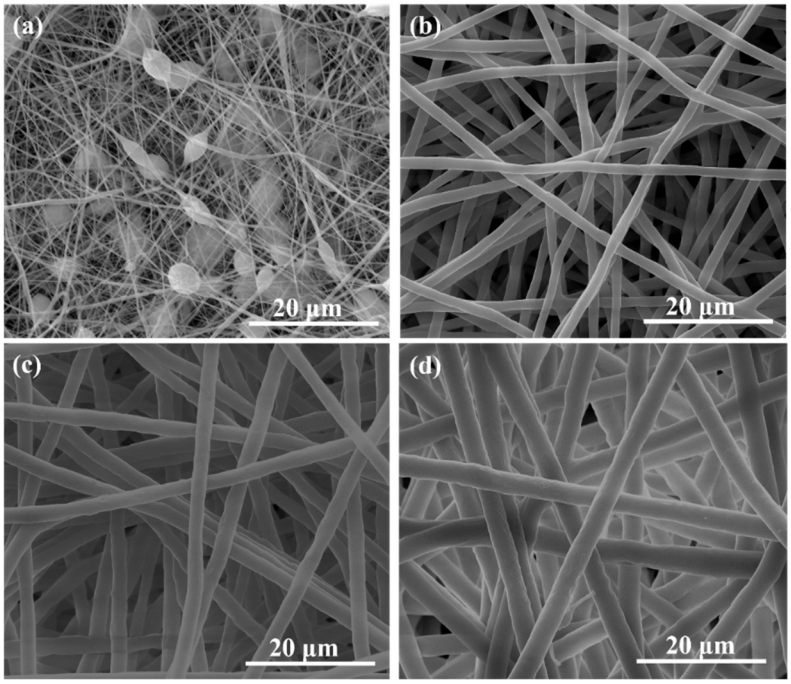

Figure 1. SEM images obtained from a scanning electron microscope reveal the structure of PCL nanofibers produced through electrostatic spinning:(a) F1, (b) F2, (c) F3, and (d) F4.

Subsequently, we examined the effects of different concentrations of n-ZnO on fiber morphology to determine the optimal drug loading. As depicted in Figure 2 (a-d), 0.5%, 1%, 2%, and 3% n-ZnO were incorporated into a 10% PCL solution, respectively. SEM images revealed that fibers containing 1% n-ZnO (F6) began to exhibit bending. Moreover, as the concentration of n-ZnO increased, the protrusions of particles became more pronounced, which could even lead to non-uniform fiber diameters. Based on these observations, fibers with a drug loading of 0.5% n-ZnO (F5) were selected for further experiments.

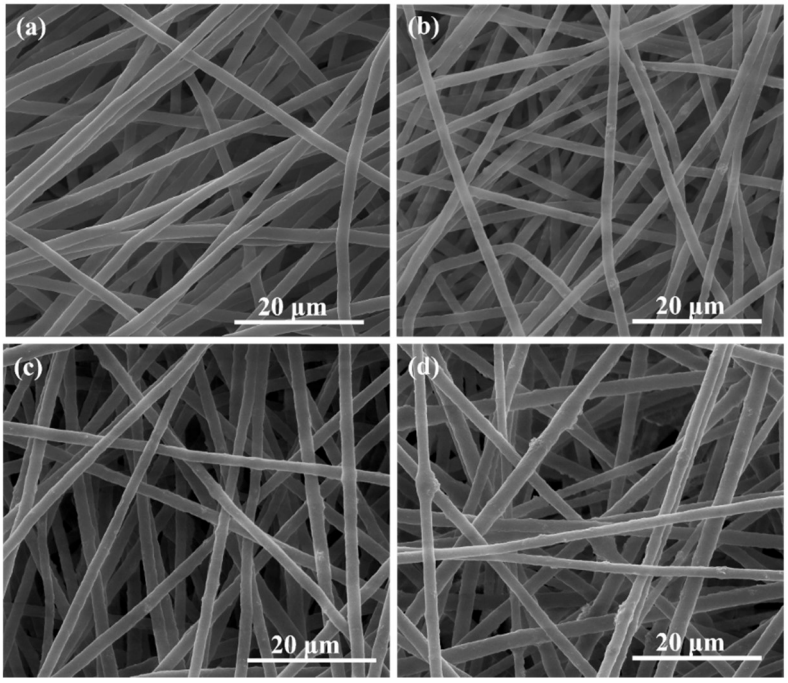

Figure 2. SEM images of 10% PCL loaded with varying compositions of n-ZnO. (a) F5, (b) F6, (c) F7, and (d) F8.

ISSN: 2414-1895 DOI: 10.6919/ICJE.202505_11(5).0034

Next, as illustrated in Figure 3 (a-d), we investigated the effects of different PCL-gelatin ratios on fiber morphology. In Figure 3 (a), when the PCL-gelatin ratio was 6:4, the F9 fibers were irregular overall, with uneven thickness and the presence of fine particles, numerous thin filaments, and mesh-like materials. As the PCL-gelatin ratio changed to 7:3 (Figure 3 (b)), the mesh-like materials in F10 gradually decreased, but thin filaments and uneven fibers still existed. When the ratio was adjusted to 8:2, the diameter of F11 fibers became more uniform, although thin filaments were still present. However, when the PCL-gelatin ratio increased to 9:1, the F12 fibers became twisted again, with significant differences in fiber appearance and a noticeable reduction in diameter, accompanied by an increase in thin filaments. Therefore, F11 fibers were selected for further discussion.

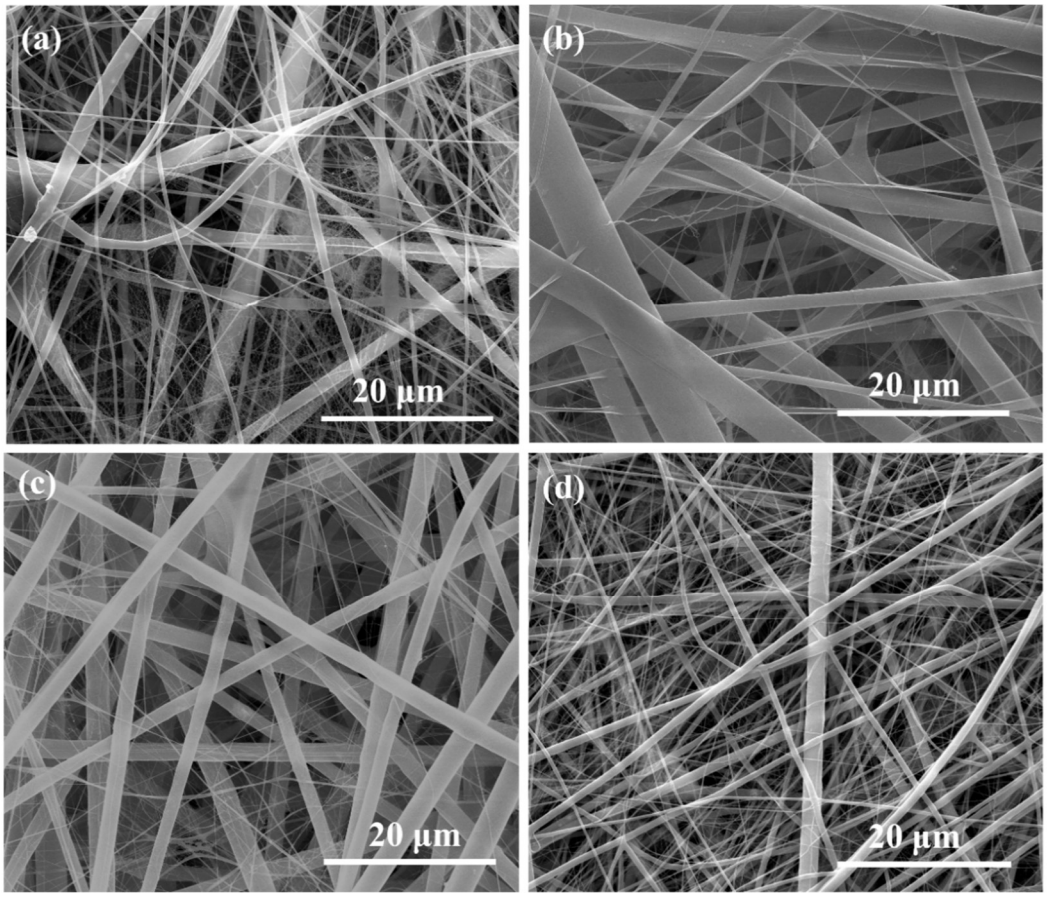

Figure 3. SEM images of single-fluid electrospun fibers with different PCL-gelatin ratios: (a) F9; (b) F10; (c) F11; (d) F12.

3.2 Morphological Analysis of Coaxial Electrospun Nanofibers

After determining the spinning window for single-fluid electrospinning and the proportion of the loaded substance, this study further conducted coaxial electrospinning experiments to explore the effects of different concentrations and flow rate ratios of the core and shell fluids on the spinning process and fiber morphology. The experimental parameters are shown in Table 1. When only the concentration of PCL in the core and shell layers was changed while the feeding rate remained consistent, the fiber morphology could be observed as shown in Figure 4 (a and b). When the core layer concentration was lower than the shell layer concentration, the F13 fibers in Figure 4 (a) appeared crimped, with many fibers adhering to each other. In contrast, when the core layer concentration was higher than the shell layer concentration, the F14 fibers had a smooth surface and uniform diameter distribution without crimping. Therefore, the concentration of the core layer for coaxial electrospun fibers was determined to be 15% PCL, and the shell layer concentration was set at 10% PCL.

ISSN: 2414-1895 DOI: 10.6919/ICJE.202505_11(5).0034

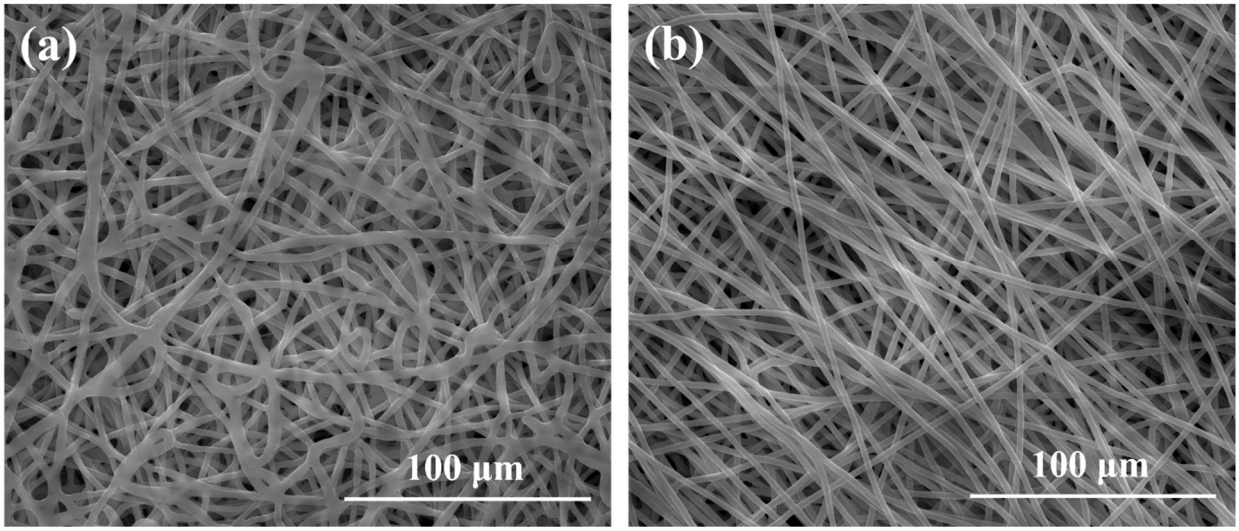

Figure 4. SEM images of coaxial electrostatically spun PCL nanofibres with different concentration gradients and same flow rate:(a) F13, and (b) F14.

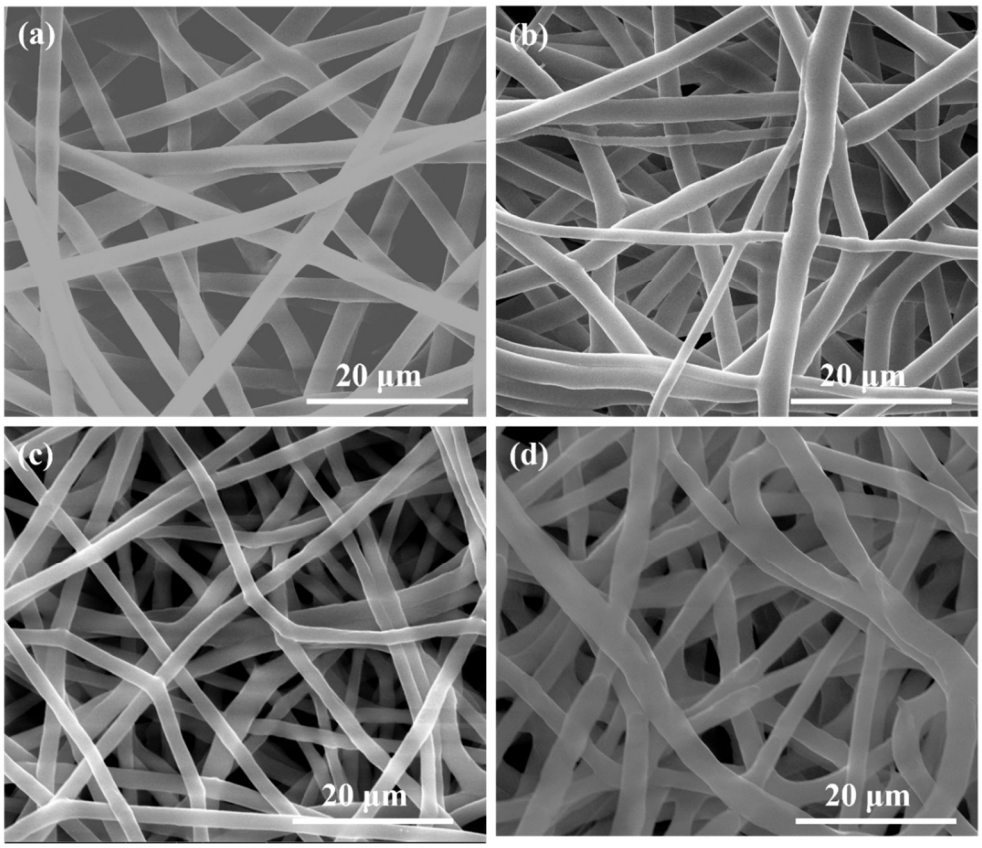

Figure 5. SEM images of coaxial composite PCL nanofibres with the same concentration gradient and different flow rate ratios:(a) F15, (b) F16, (c) F17, and (d) F18.

After establishing the core layer concentration at 15% PCL and the shell layer concentration at 10% PCL, we further investigated the effects of different flow rates of the core and shell fluids on the electrospinning process and fiber morphology, with the results shown in Figure 5 (a-d). When the flow rate ratio of the core to shell fluid was 0.5:1.0, the F15 fibers exhibited a smooth surface without particles and a uniform diameter distribution. However, when the flow rate ratio was 0.5:1.5, the F16 fibers began to show bending due to stretching, leading to the appearance of fibers with smaller diameters. When the flow rate ratio was adjusted to 1.0:0.5, the degree of bending in the F17 fibers

ISSN: 2414-1895 DOI: 10.6919/ICJE.202505_11(5).0034

increased, and the fiber diameter was significantly reduced compared to that in Figure 5 (a). In contrast, when the flow rate ratio was 1.5:0.5, the F18 fibers in Figure 5 (d) exhibited more severe bending and a noticeable increase in fiber diameter. Therefore, the best fiber morphology was achieved with the core-to-shell flow rate ratio of 0.5:1.0, as seen in the F15 fibers.

4. Conclusion

This article investigates the morphology of electrospun nanofibers based on PCL under various processing parameters and additives. Systematic studies indicate that solution concentration primarily governs fiber diameter and the formation of defects. Additionally, the concentration and feed rate differences within the core-shell layer of a co-axial electrospinning system significantly affect fiber uniformity and branching behavior. Optimizing flow rates is crucial for maintaining stable jet formation, and the precise introduction of additives can finely tune the fiber surface morphology and diameter distribution. Identifying the synergistic effects among parameters enables the production of defect-free fibers with customized morphologies, advancing fundamental understanding of electrospinning dynamics and providing a foundation for designing PCL nanofibers tailored for specific applications.

Acknowledgments

The authors would like to acknowledge the National Natural Science Foundation of China (NNSFC) (Grant No. 51201107) for financial support.

References

[1] A. Greiner and J. H. Wendorff. Electrospinning: a fascinating method for the preparation of ultrathin fibers, Angewandte Chemie, International Edition in English, vol. 46 (2007), 5670-5703.

[2] X. Yan, M. Yu, W.-P. Han, et al. Fabrication and formation mechanism of closed-loop fibers by electrospinning with a tip collector, Chinese Physics B, vol. 25 (2016).

[3] T. Ghosh, T. Das and R. Purwar. Review of electrospun hydrogel nanofiber system: Synthesis, Properties and Applications, Polymer Engineering & Science, vol. 61 (2021), 1887-1911.

[4] X. Zhang, X. Shi, J. E. Gautrot, et al. Nanoengineered electrospun fibers and their biomedical applications: a review, Nanocomposites, vol. 7 (2020), 1-34.

[5] T. U. Rashid, R. E. Gorga and W. E. Krause. Mechanical Properties of Electrospun Fibers-A Critical Review, Advanced Engineering Materials, vol. 23 (2021).

[6] P. J. Rivero, D. Yurrita, C. Berlanga, et al. Functionalized Electrospun Fibers for the Design of Novel Hydrophobic and Anticorrosive Surfaces, Coatings, vol. 8 (2018).

[7] P. Mandal and R. Shunmugam. Polycaprolactone: a biodegradable polymer with its application in the field of self-assembly study, Journal of Macromolecular Science, Part A, vol. 58 (2020), 111-129.

[8] T. Khatti, H. Naderi-Manesh and S. M. Kalantar. Application of ANN and RSM techniques for modeling electrospinning process of polycaprolactone, Neural Computing and Applications, vol. 31 (2017), 239-248.

[9] V. T. Kimura, M. H. A. Zanin and S. H. Wang. Influence of thickness on the properties of electrospun PCL/gelatin nanofiber scaffolds, Polymer Bulletin, vol. 81 (2024), 9347-9361.

[10] M. F. Hossain, R. H. Gong and M. Rigout. Effect of polymer concentration on electrospinning of hydroxypropyl-β-cyclodextrins/PEO nanofibres, The Journal of The Textile Institute, vol. 107 (2016), 1511-1518.

[11] C. Sun, C. Ayranci, Y. Chen, et al. Can Extensional Flow Rupture Macromolecules in an Electrospinning Process?, Journal of Polymer Science Part B: Polymer Physics, vol. 55 (2017), 1051-1054.

[12] J. d. D. P. d. Moraes Segundo, M. Oneide Silva de Moraes, W. R. Brito, et al. Incorporation of molecularly imprinted polymer nanoparticles in electrospun polycaprolactone fibers, Materials Letters, vol. 275 (2020).

[13] M. Wildy, W. Wei, K. Xu, et al. Heat's Role in Solution Electrospinning: A Novel Approach to Nanofiber Structure Optimization, Langmuir, vol. 40 (2024), 7982-7991.